ISSN 1070-4280, Russian Journal of Organic Chemistry, 2019, Vol. 55, No. 6, pp. 866–873. © Pleiades Publishing, Ltd., 2019.

A Novel Fluorescent Probe Based on Spiro[chromeno[2,3-*c*]pyrazole-4,1′-[2]benzofuran]-3′-one for Detecting Copper(II) ions in Aqueous Solution

Yongshuang Yue[a], Zhengfeng Xie[a],* Yicheng Chu[a], and Wei Shi[a]

[a] *Oil & Gas Field Applied Chemistry Key Laboratory of Sichuan Province, College of Chemistry and Chemical Engineering, Southwest Petroleum University, Chengdu, China*
**e-maul: xiezhf@swpu.edu.cn*

Received December 27, 2018; revised February 21, 2019; accepted April 25, 2019

Abstract—A novel fluorescent probe, **DHMP** {7-(dibutylamino)-3-methyl-1*H*,3′*H*-spiro[chromeno[2,3-*c*]pyrazole-4,1′-[2]benzofuran]-3′-one} was designed and synthesized by condensation of 2-[4-(dibutylamino)-2-hydroxybenzoyl]benzoic acid with 5-methyl-2,4-dihydropyrazol-3-one. The ultraviolet absorption and fluorescence emission spectra of **DHMP** showed a clear pH dependence and highly selective and sensitive response to copper(II) ions in aqueous medium. The detection limit of Cu^{2+} was estimated at 9.05×10^{-8} M.

Keywords: 1,4-dihydrochromeno[2,3-*c*]pyrazole, 7-(dibutylamino)-3-methyl-1*H*,3′*H*-spiro[chromeno[2,3-*c*]-pyrazole-4,1′-[2]benzofuran]-3′-one, fluorescent probe, copper ion detection, pH, aqueous medium.

DOI: 10.1134/S1070428019060186

Copper is an essential trace element in the human body. It is widely distributed in biological tissues, mostly in organic complexes such as metalloproteins which play a functional role in the form of enzymes [1–4]. Copper deficiency in a body will induce such diseases as anemia, arthritis, brain dysfunction, and leucodermia [5, 6]. In contrast, excessive intake of copper will also lead to a variety of diseases, including Alzheimer's, Parkinson's, and Wilson's diseases [7–9]. Therefore, convenient, fast, and reliable methods for the detection of Cu^{2+} in drinking water and foods are important and necessary.

In recent years, many methods have been developed for detecting Cu^{2+} on the basis of fluorescence, stripping voltammetry, atomic absorption spectrometry (AAS), inductively coupled plasma optical emission spectrometry (ICP-OES), and colorimetry [10, 11]. Compared with these traditional technologies, fluorescent probes have more advantages for the detection of Cu^{2+} due to simplicity, good selectivity, high sensitivity, and great potential for bioimaging [12–16]. Up to date, a great number of fluorescent probes for the detection and recognition of Cu^{2+} have been designed and synthesized [17]. Several commonly known fluorophores, such as coumarin [18], BODIPY [19], fluorescein [20], pyrene [21], and rhodamine [8] are frequently used to construct these probes. But a simple and efficient approach to detection of Cu^{2+} ions still involves many challenges. Therefore, it is very necessary to design and synthesize a new probe to solve these problems.

In recent years, our group has successfully synthesized a series of fluorescent probes that selectively recognize mercury [22–24], aluminum [25], copper [26], and cyanide ions [27]. A novel probe for cyanide ions, 7-(dibutylamino)-2′-[(2-hydroxybenzylidene)-amino]-3-methyl-1-phenyl-1*H*-spiro[chromeno[2,3-*c*]-pyrazole-4,1′-isoindol]-3′-one (**SCPZ-S**), has been synthesized from 5-methyl-2-phenyl-2,4-dihydropyrazol-3-one [28]. However, all these probes have the same drawback due to their poor solubility in water. Therefore, in this work we used 5-methyl-2,4-dihydro-3*H*-pyrazol-3-one to design and synthesize a novel fluorescent probe, **DHMP**. Unlike rhodamine and fluorescein

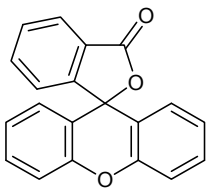

A

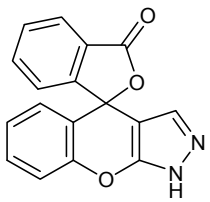

DHMP

which have xanthene structure **A**, **DHMP** has the 1,4-dihydrochromeno[2,3-*c*]pyrazole fragment. The presence of an active hydrogen on the pyrazole ring affects the properties of **DHMP**. This completely asymmetrical structure has more possibilities for its internal electronic arrangement and migration, which may increase its complexing and recognizing ability for specific ions. The ultraviolet absorption and fluorescence emission spectra of **DHMP** obviously change with respect to the acidity of the medium. In addition, it exhibited good selective fluorescent response to Cu^{2+} in aqueous media.

EXPERIMENTAL

All reagents and solvents, in particular 2-[4-(dibutylamino)-2-hydroxybenzoyl]benzoic acid, anhydrous ethanol, concentrated sulfuric acid, and hydrazine hydrate, were purchased from Adams and Acros Chemical Co. and were used without purification. All inorganic salt solutions were prepared from distilled water to afford a concentration of 0.1 M. **DHMP** was dissolved in dimethyl sulfoxide to a concentration of 10^{-3} M.

The ^{1}H NMR and ^{13}C NMR spectra were recorded on a Varian Inova-400 spectrometer at 400 and 100 MHz, respectively, using chloroform-*d* as solvent. The electronic absorption spectra were recorded using a Metash UV-6000PC UV-vis spectrometer. The emission spectra were recorded on an F-320 (Gangdong Technology) fluorescence spectrometer. The high resolution mass spectra were obtained on a Waters Q-TOF Premier instrument.

7-(Dibutylamino)-3-methyl-1*H*,3′*H*-spiro[chromeno[2,3-*c*]pyrazole-4,1′-[2]benzofuran]-3′-one (DHMP). A mixture of 0.369 g (1 mmol) of 2-[4-(dibutylamino)-2-hydroxybenzoyl]benzoic acid, 0.098 g (1 mmol) of 5-methyl-2,4-dihydro-3*H*-pyrazol-3-one, and 4 mL of concentrated sulfuric acid was stirred for 7 h at 100°C. The mixture was cooled to room temperature and poured into ice water, and the yellow precipitate was collected by vacuum filtration. The crude product was purified by column chromatography using ethyl acetate–petroleum ether (1:3 by volume) as eluent. Yield 50%, pale yellow solid, mp 204–207°C. ^{1}H NMR spectrum, δ, ppm: 8.00 d (1H, *J* = 4 Hz), 7.66 t (1H, *J* = 16 Hz), 7.59 t (1H, *J* = 12 Hz), 7.26 s (1H), 7.2 d (1H, *J* = 8 Hz), 6.57 d (1H, *J* = 8 Hz), 6.41 d (1H, *J* = 4 Hz), 6.32 d.d (1H, *J* = 4, 4 Hz), 3.25 t (4H, *J* = 16 Hz), 1.72 s (3H), 1.55 m (4H), 1.33 m (4H), 0.94 t (6H, *J* = 12 Hz). ^{13}C NMR spectrum, δ_C, ppm: 169.66, 158.17, 153.49, 152.28, 149.91, 138.16, 134.81, 129.47, 128.80, 126.90, 124.79, 123.73, 108.43, 105.38, 98.45, 96.74, 83.27, 50.79, 29.27, 20.26, 13.95, 10.34. IR spectrum, ν, cm^{-1}: 2954, 2867, 1756, 1614, 1498, 1257, 1112, 755. Mass spectrum (TOF-MS+): *m*/*z* 432.2182 $[M + H]^+$. $C_{26}H_{30}N_3O_3$. Calculated: *M* + H 432.2282.

RESULTS AND DISCUSSION

The new fluorescent probe, 7-(dibutylamino)-3-methyl-1*H*,3′*H*-spiro[chromeno[2,3-*c*]pyrazole-4,1′-[2]benzofuran]-3′-one (**DHMP**) was synthesized in 50% yield by heating equimolar amounts of 2-[4-(dibutylamino)-2-hydroxybenzoyl]benzoic acid and 5-methyl-2,4-dihydro-3*H*-pyrazol-3-one in concentrated sulfuric acid at 100°C for 7 h (Scheme 1) and was purified by chromatography.

To evaluate the potential applications of probe for the detection of pH, the pH effects on the fluorescence and UV-Vis absorption spectra of **DHMP** (10 μM) were studied. Figure 1a shows that the fluorescence emission of **DHMP** enhances gradually with a blue shift in the pH range 1.1–13.9. The absorption spectra of **DHMP** exhibited two maxima at λ 475 and 503 nm in the pH range 1.0–6.1. However, in the pH range from 6.9 to 9.1, the absorption peak at λ 503 nm gradually decreases up to complete disappearance, and only one absorption peak is observed in the pH range 9.1–13.9. The blue shift and disappearance of the absorption peak at λ 503 nm are more obvious in the pH range 7.4–8.8. A detailed examination was carried out studied with a pH gradient of 0.2, and the result is shown in Fig. 1c.

Scheme 1.

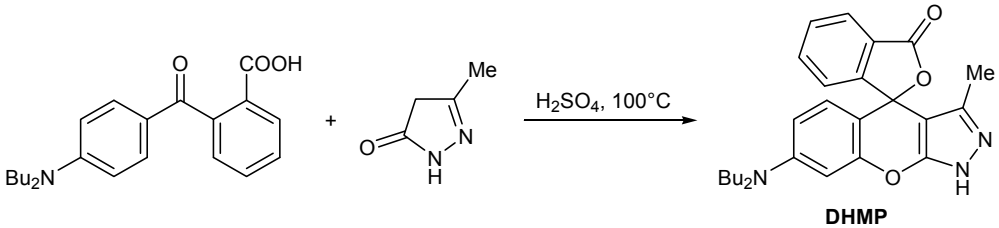

DHMP

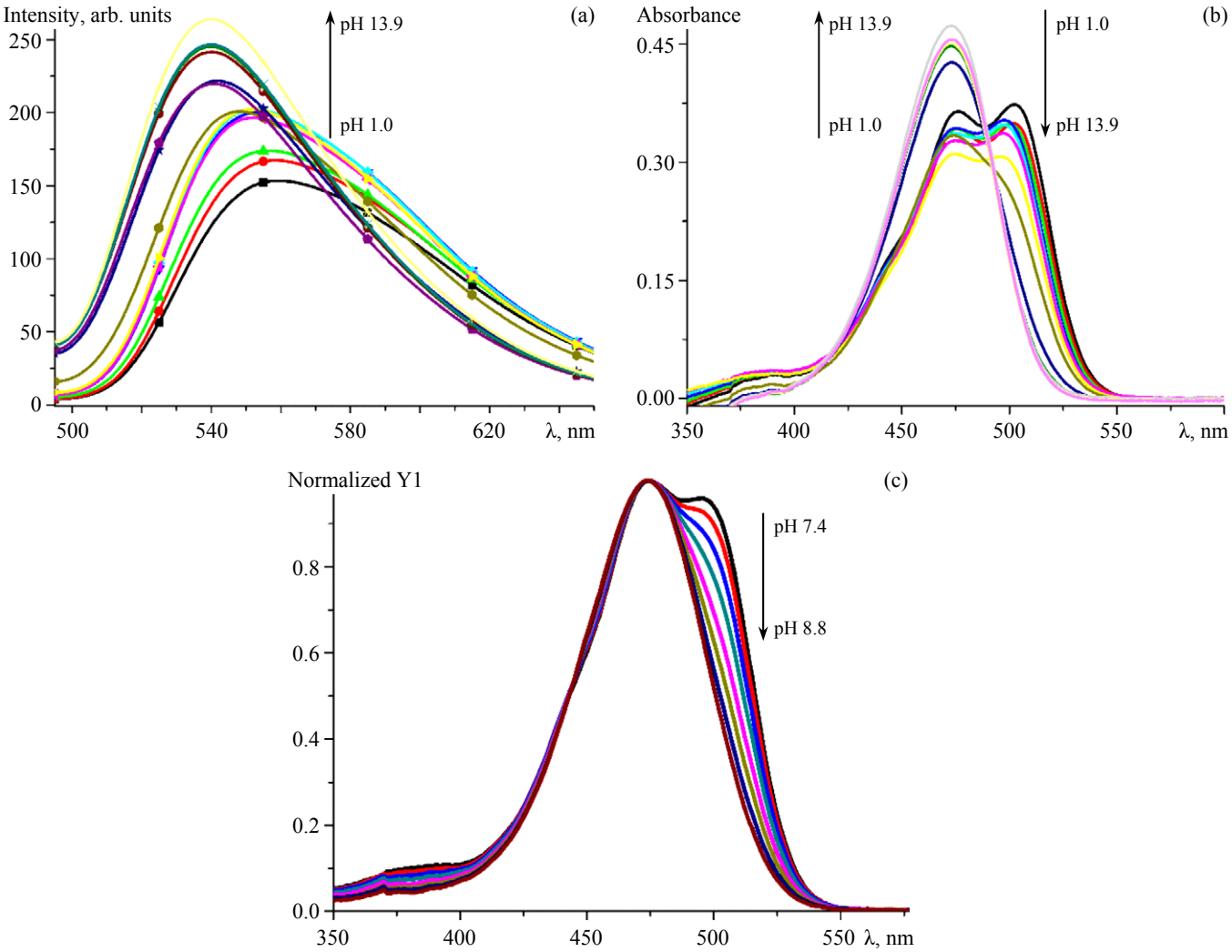

Fig. 1. (a) Fluorescence spectra (λ_{excit} 475 nm) of a solution of **DHMP** (10 μM) in a buffer (5 mM) at different pH values; (b) electrnic absorption spectra of **DHMP** (10 μM) in a buffer (5 mM) at different pH values; (c) electronic absorption spectra of **DHMP** (10 μM) in a buffer (5 mM) in the pH range 7.4–8.8.

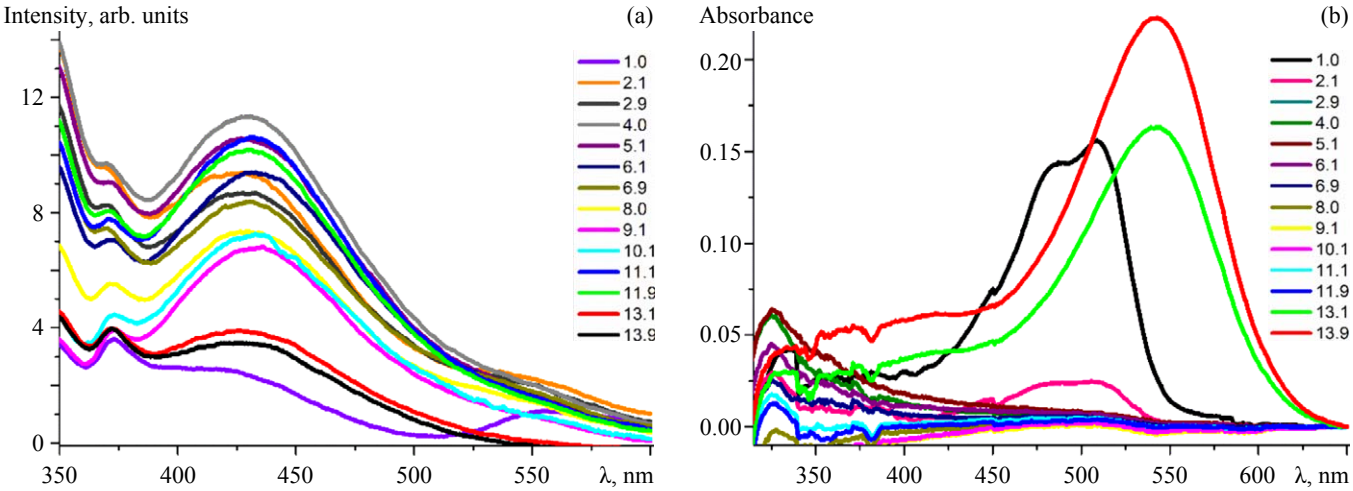

Fig. 2. (a) Fluorescence spectra (λ_{excit} 323 nm) of **DHMB** (10 μM) in a buffer solution (5 mM) at different PH values; (b) electronic absorption spectra of **DHMB** (10 μM) in a buffer solution (5 mM) at different pH values.

To evaluate a possible response mechanism of **DHMP** for pH, we have synthesized its structural analog, 7-(dibutylamino)-3-methyl-1-phenyl-1*H*,3′*H*-spiro[chromeno[2,3-*c*]pyrazole-4,1′-[2]benzofuran]-3′-one (**DHMB**) as shown in Scheme 2. The effects of pH on the fluorescence and UV-Vis absorption spectra of **DHMB** (10 μM) are illustrated by Fig. 2. In the pH range from 2.9 to 11.9, there was no significant change in the absorption pattern. In strongly acidic (pH 1.1–2.1) or strongly alkaline medium (13.1–13.9), an absorption band appeared at λ 510 nm or 550 nm, respectively. However, there was no significant fluorescence in the pH range from 1.1 to 13.9. Comparison of the structures of **DHMP** and **DHMB** suggest that the most probable reason for the observed difference in their spectral behavior is not ring opening but protonation of the nitrogen atom. A possible response mechanism is shown in Scheme 3. In neutral system, there is an equilibrium between two NH forms. As the pH value decreases, **DHMP** molecule is protonated at the dibutylamino nitrogen atom. Under strongly alkaline conditions, deprotonation of the pyrazole ring occurs to form sodium salt. Thus, protonation and deprotonation of the dibutylamino and pyrazole nitrogen atoms, respectively, are responsible for the sensitivity of **DHMP** to variation of pH.

The fluorescence spectra of **DHMP** were measured in water–DMSO mixtures at different proportions. The probe is readily soluble in DMSO, and its solutions in that solvent showed no fluorescence (Fig. 3). However, as the fraction of water increased, the fluorescence emission intensity gradually increased.

An important feature of the probe is that it exhibited selectivity for Cu^{2+} over other metal ions. Figure 4 shows the fluorescence spectral changes upon addition of various metal ions (10 equiv) in HEPES buffer (20 mM, pH 7.4)/DMSO (99:1, v/v), including Ag^{+}, Ba^{2+}, Ca^{2+}, Cd^{2+}, Co^{2+}, Cr^{3+}, Fe^{3+}, Hg^{2+}, K^{+}, Mg^{2+}, Na^{+}, Ni^{2+}, Pb^{2+}, and Zn^{2+}; all these ions caused very minor changes. However, the probe displayed obvious fluorescence quenching at λ 552 nm in the presence of

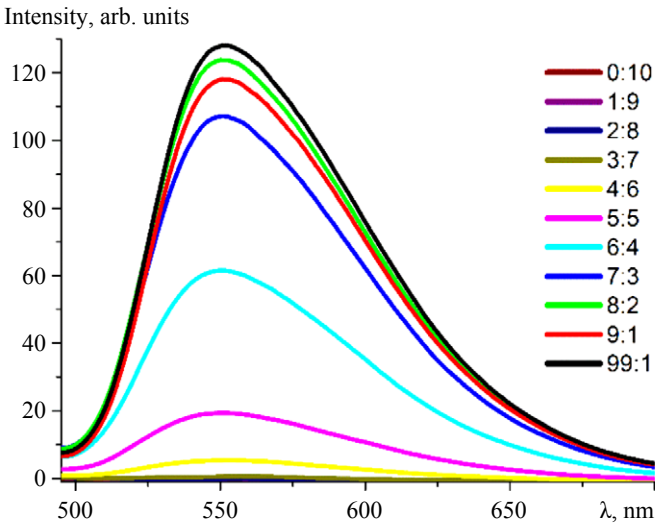

Fig. 3. Fluorescence spectra (λ_{excit} 475 nm) of **DHMP** (10 μM) in water–DMSO mixtures at different proportions.

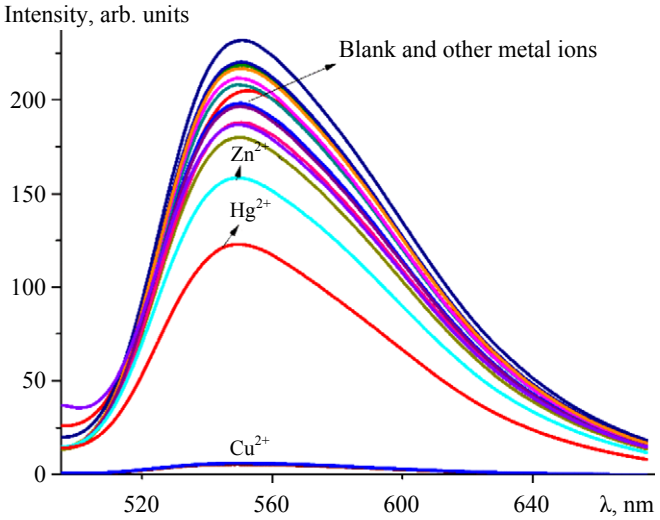

Fig. 4. Fluorescence spectra (λ_{excit} 475 nm) of **DHMP** (10 μM) in HEPES buffer (20 mM, pH 7.4)/DMSO (99:1) in the presence of various metal ions.

Cu^{2+}. Good selectivity for Cu^{2+} over other competing metal ions is an important parameter characterizing **DHMP** as a probe. Hence, the effect of competing metal ions was studied. Competitive experiments were

Scheme 2.

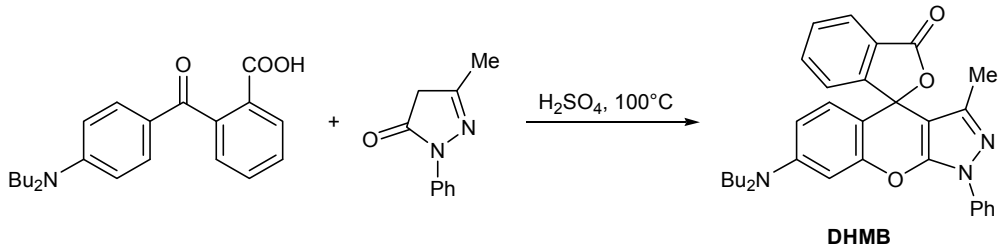

DHMB

Scheme 3.

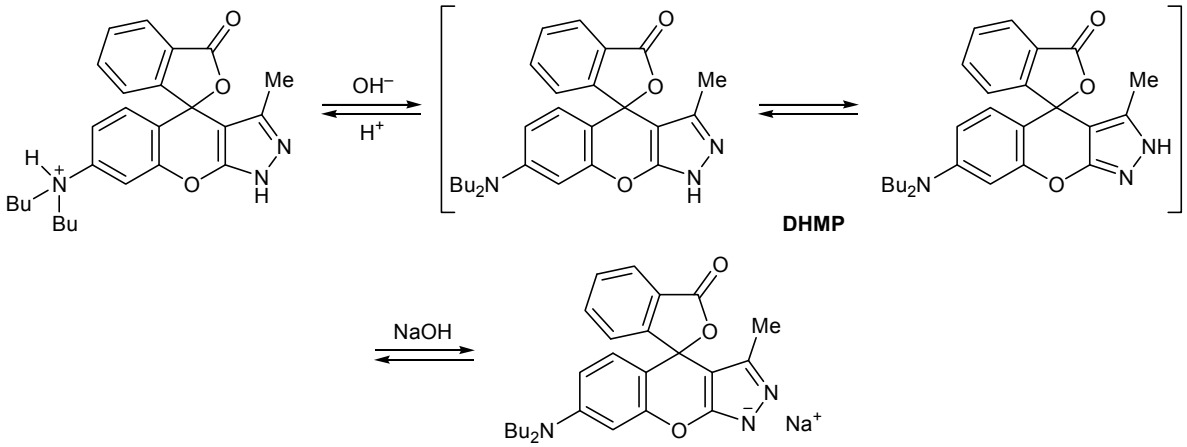

carried out using 10 equiv of interfering metal ions in the presence of 10 equiv of Cu^{2+}. As shown in Fig. 5, there are no significant variations in the fluorescence emission spectrum at λ 552 nm in the presence of other interfering metal ions. It is worth noting that Hg^{2+} also showed no significant effect on the fluorescence spectra, indicating that **DHMP** has a good selectivity for Cu^{2+} over other metal ions. Thus, **DHMP** can be used as a selective fluorescence sensor for Cu^{2+}.

The properties of **DHMP** with Cu^{2+} in H_2O–DMSO (99:1, v/v; HEPES buffer, 20 mM, pH 7.4) were further studied using fluorescence titration. As shown in Fig. 6, free **DHMP** (10 μM) displayed a notable fluorescence emission peak at λ 552 nm. However, upon addition of Cu^{2+} (0–250 μM) to a solution of **DHMP**, the fluorescence intensity at λ 552 nm significantly decreased and gradually reached a minimum when 100 μM of Cu^{2+} was added. Over 10-fold reduction of the fluorescence intensity was observed under saturation conditions.

The detection limit of **DHMP** for Cu^{2+} was also calculated based on the fluorescence titration data. The fluorescence emission spectrum of **DHMP** was measured 10 times, and the standard deviation of the blank measurement was then calculated. To obtain the slope, the ratio of the fluorescence intensity at λ 552 nm was plotted versus the Cu^{2+} concentration (Fig. 7). The detection limit (DL) was calculated by the formula

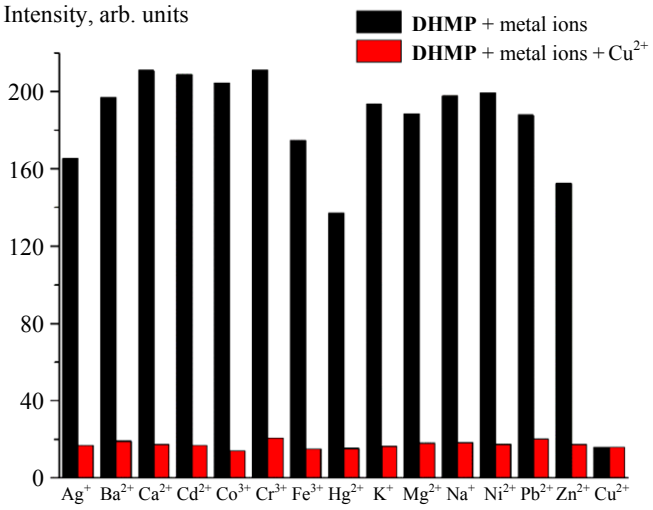

Fig. 5. Variation of fluorescence intensity of **DHMP** (10 μM) upon addition of various metal ions (100 μM) in the presence of Cu^{2+} (100 μM). Black bars represent the fluorescence response of **DHMP** and competing ions. Red bars correspond to the subsequent addition of 100 μM Cu^{2+} to the above solutions.

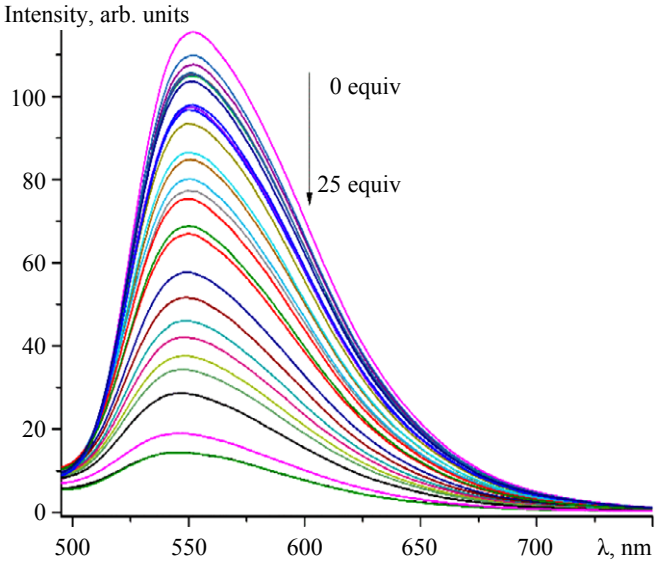

Fig. 6. Fluorescence spectra (λ_{excit} 475 nm) of **DHMP** (10 μM) in HEPES buffer (20 mM, pH 7.4)/DMSO (99:1, v/v) in the presence of different amounts of Cu^{2+} ions (0–250 μM).

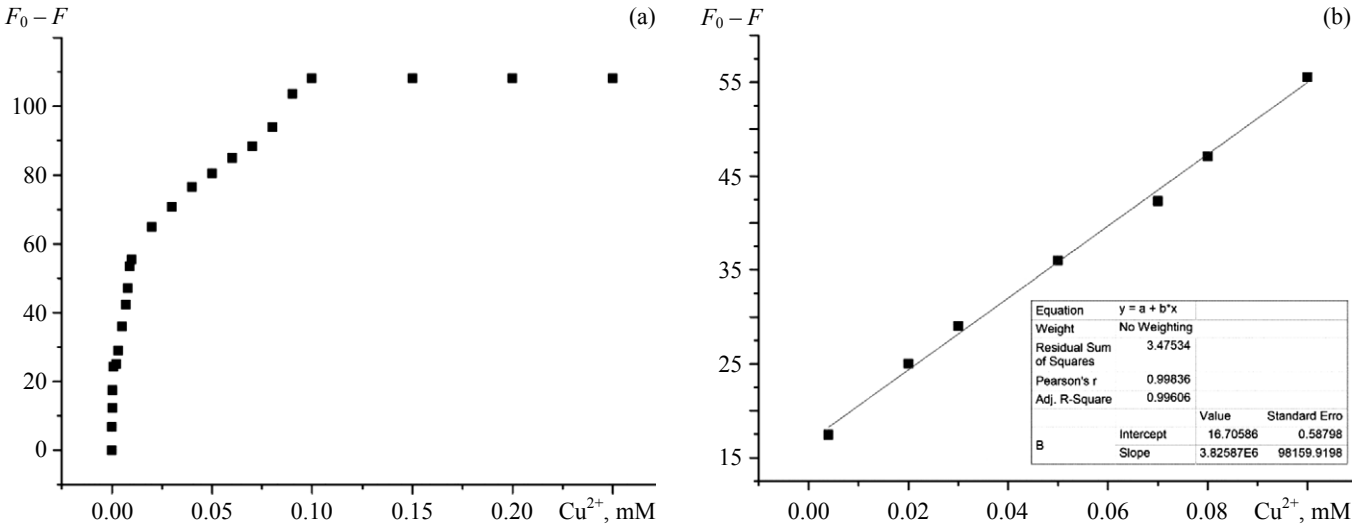

Fig. 7. (a) Variation of the fluorescence intensity (λ 552 nm) of **DHMP** (10 μM) in HEPES buffer (20 mM, pH 7.4)/DMSO (99 : 1, v/v) in the presence of different amounts of Cu^{2+} ions (0–140μM); (b) linearity of fluorescent response between 0 and 10 μM Cu^{2+}.

DL = 3σ/*K*, where σ is the standard deviation of the blank and *K* is the slope of the calibration curve. Thus, the detection limit was estimated at 9.05×10^{-8} M.

The stoichiometry calculations for [Cu^{2+}]–**DHMP** were performed by means of a Job plot which was generated by varying the mole fraction of Cu^{2+} from 0 to 1.0 in a Cu^{2+}–**DHMP** solution with a total concentration of 10 μM, and the decrease of the fluorescence intensity was measured. As shown in Fig. 8, the fluorescence drop at λ 552 nm had a maximal increment at a Cu^{2+} mole fraction of 0.5, indicating a 1 : 1 stoichiometry. The stoichiometric ratio of **DHMP** to Cu^{2+} was also confirmed by the mass spectral data (supporting information is available from the authors).

Likewise, Cu^{2+} was added to a solution of **DHMB** (10 μM) in HEPES buffer (20 mM, pH 7.4)/DMSO (99 : 1) to study the effect on the fluorescence spectra. Figure 9 shows that there was no significant fluorescence quenching. Comparison of the structures and fluorescence emission spectra of **DHMP** and **DHMB** suggests that the fluorescence quenching is not the result of ring opening. A plausible mechanism of **DHMP** sensing for Cu^{2+} is illustrated by Scheme 4.

Scheme 4.

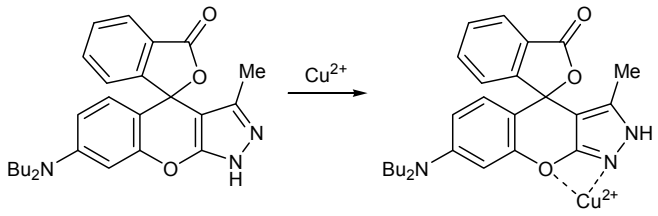

To show potential applicability of **DHMP** for analysis of real samples, water samples were collected from lake water, tap water, and distilled water. After removal of solid particles by filtration, each sample was mixed with HEPES buffer (20 mM, pH 7.4, 1 : 1 v/v) and subjected to analysis of Cu^{2+} with the probe. The fluorescence responses of **DHMP** (10 μM) toward these water samples were examined directly or spiked with different concentrations of Cu^{2+} (0, 0.5, 1.0, 5.0, and 10.0 equiv), respectively. The results are shown in Fig. 10; similar responses to Cu^{2+} were observed for all samples. This result indicates potential applicability of **DHMP** for the detection of Cu^{2+} in real water samples.

In summary, we have designed and synthesized a novel fluorescent probe, **DHMP**, selective for Cu^{2+}

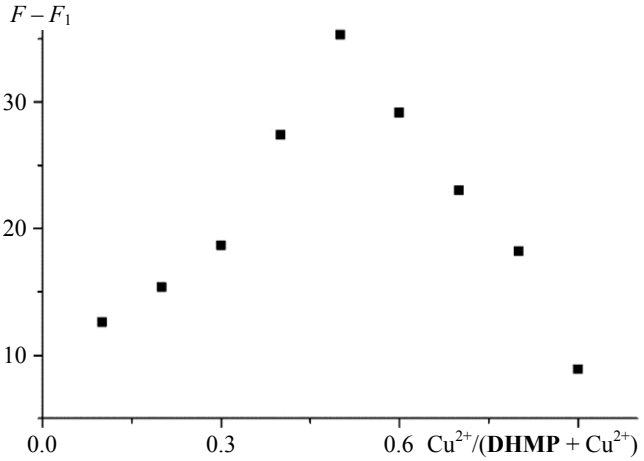

Fig. 8. Job's plots according to the continuous variation method; overall concentration of **DHMP** and Cu^{2+} 10 μM.

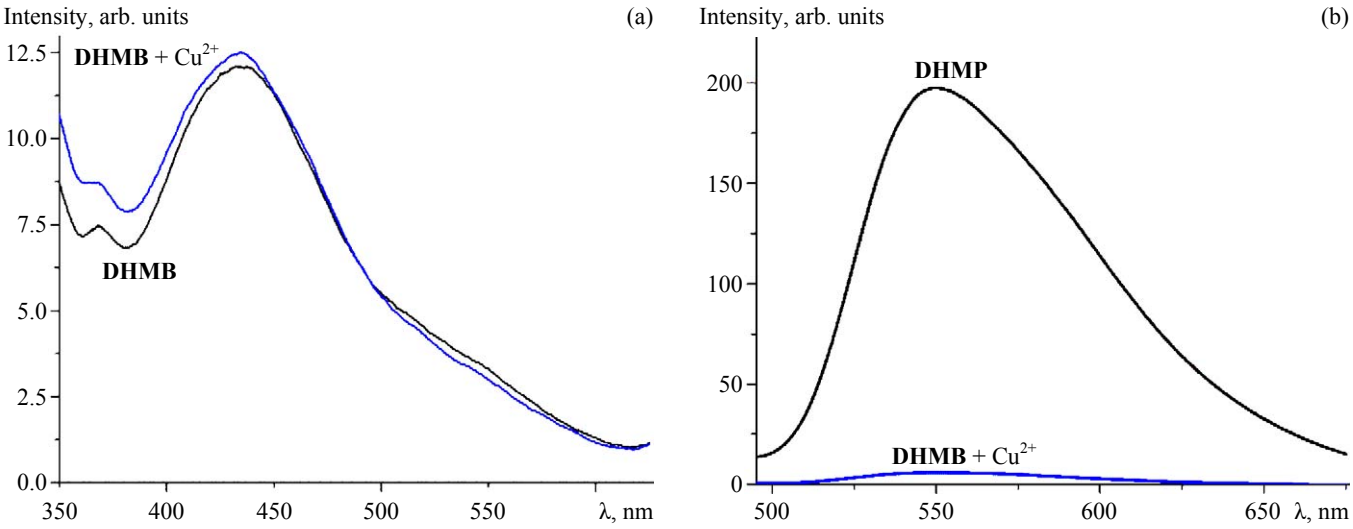

Fig. 9. (a) Fluorescence spectra (λ_{excit} 326 nm) of **DHMB** (10 μM) in HEPES buffer (20 mM, pH 7.4)/DMSO (99 : 1, v/v) in the presence of Cu^{2+} ions; (b) fluorescence spectra (λ_{excit} 475 nm) of **DHMP** (10 μM) in HEPES buffer (20 mM, pH 7.4)/DMSO (99 : 1, v/v) in the presence of Cu^{2+} ions.

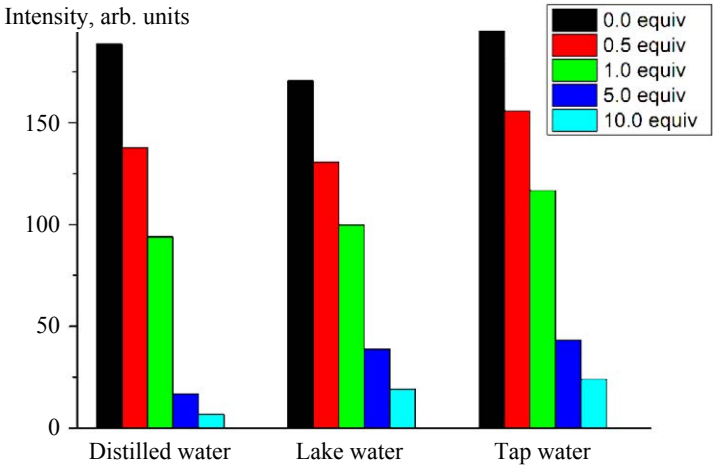

Fig. 10. Fluorescence intensities at λ 552 nm of solutions containing **DHMP** and different amounts of Cu^{2+} ions (0–10 equiv) in distilled water, lake water, and tap water/HEPES buffer (20 mM, pH 7.4, 1 : 1, v/v).

over other metal ions with high sensitivity (detection limit 9.05×10^{-8} M).

CONFLICT OF INTERESTS

The authors declare the absence of conflict of interests.

REFERENCES

1. Zhu, D., Luo, Y., Shuai, L., Xie, W., Yan, X., Duan, Z., and Cai, W., *Tetrahedron Lett*., 2016, vol. 57, no. 48, p. 5326.
2. Liu, S., Liu, Y., Pan, H., Chen, H. and Li, H., *Tetrahedron Lett*., 2018, vol. 59, no. 2, p. 108.
3. Li, Y., Sun, M., Zhang, K., Zhang, Y., Yan, Y., Lei, K., Wu, L., Yu, H., and Wang, S., *Sens. Actuators, B*, 2017, vol. 243, p. 36.
4. Cheng, D., Liu, X., Yang, H., Zhang, T., Han, A., and Zang, L., *Sensors*, 2017, vol. 17, no. 1, p. 35.
5. Barnham, K.J., Masters, C.L., and Bush, A.I., *Nat. Rev. Drug Discovery*, 2004, vol. 3, no. 3, p. 205.
6. Bourassa, M.W. and Miller, L.M., *Metallomics*, 2012, vol. 4, no. 8, p. 721.
7. Peng, D., Hu, B., Kang, M., Wang, M., He, L., Zhang, Z., and Fang, S., *Appl. Surf. Sci*., 2016, vol. 390, p. 422.
8. Xu, L., Wei, S., Diao, Q., Ma, P., Liu, X., Sun, Y., Song, D., and Wang, X., *Sens. Actuators, B*, 2017, vol. 246, p. 395.
9. Ren, D., Liu, Y., Liu, X., Li, Z., Li, H., and Yang, X.F., *Sens. Actuators, B*, 2017, vol. 255, p. 2321.

10. Gu, B., Huang, L., Su, W., Duan, X., Li, H., Yao, S., *Anal. Chim. Acta*, 2017, vol. 954, p. 97.
11. Shen, Y., Zhang, X., Zhang, C., Zhang, Y., Jin, J., and Li, H., *Spectrochim, Acta, Part A*, 2017, vol. 191, p. 427.
12. Hong, M., Lu, S., Lv, F., and Xu, D., *Dyes Pigm*., 2016, vol. 127, p. 94.
13. Long, Y., Zhou, J., Yang, M.P., Liu, X.J., Zhang, M., and Yang, B.Q., *Sens. Actuators, B*, 2016, vol. 232, p. 327.
14. Zhang, B., Diao, Q., Ma, P., Liu, X., Song, D., and Wang, X., *Sens. Actuators, B*, 2016, vol. 225, p. 579.
15. Li, C.R., Yang, Z.Y., and Li, S.L., *J. Lumin*., 2018, vol. 198, p. 327.
16. Yu, C., Wen, Y., and Zhang, J., *Sensors*, 2014, vol. 14, no. 11, p. 21375.
17. Kaewtong, C., Pulpoka, B., and Tuntulani, T., *Dyes Pigm*., 2015, vol. 123, p. 204.
18. Long, L., Wu, Y., Wang, L., Gong, A., Hu, R., and Zhang, C., *Anal. Chim. Acta*, 2016, vol. 908, p. 1.
19. Li, Z., Geng, Z.-R., Zhang, C., Wang, X.-B., and Wang, Z.-L., *Biosens. Bioelectron*., 2015, vol. 72, p. 1.
20. Xiong, X., Song, F., Wang, J., Zhang, Y., Xue, Y., Sun, L., Jiang, N., Gao, P., Tian, L., and Peng, X., *J. Am. Chem. Soc*., 2014, vol. 136, no. 27, p. 9590.
21. Li, P., He, H., Wang, Z., Feng, M., Jin, H., Yun, W., Zhang, L., Zhang, L., and Tang, X., *Anal. Chem*., 2015, vol. 88, no. 1, p. 883.
22. Lei, F., Shi, W., Ma, J., Chen, Y., Fan, K., Hui, Y., and Xie, Z., *Sens. Actuators, B*, 2016, vol. 237, p. 563.
23. Lin, H., Shi, W., Tian, Y., Ma, F., Xu, L., Ma, J., Hui, Y., and Xie, Z., *J. Lumin*., 2015, vol. 157, p. 280.
24. Shi, W., Chen, Y., Chen, X., Xie, Z., and Hui, Y., *J. Lumin*., 2016, vol. 174, p. 56.
25. Ma, J., Shi, W., Feng, L., Chen, Y., Fan, K., Hao, Y., Hui, Y., and Xie, Z., *RSC Adv*., 2016, vol. 6, no. 33, p. 28034.
26. Wang, X., Shi, W., Feng, L., Ma, J., Li, Y., Kong, X., Chen, Y., Hui, Y., and Xie, Z., *Inorg. Chem. Commun*., 2017, vol. 79, p. 50.
27. Xie, Z., Kong, X., Feng, L., Ma, J., Li, Y., Wang, X., Bao, W., Shi, W., and Hui, Y., *Sens. Actuators, B*, 2018, vol. 257, p. 154.
28. Hao, Y., Xie, Z., Bao, W., Wang, X., and Shi, W., *Chin. J. Org. Chem*., 2018, vol. 38, p. 2109.